PERGAMON

International Journal of Solids and Structures 39 (2002) 1777–1790

INTERNATIONAL JOURNAL OF SOLIDS and STRUCTURES

www.elsevier.com/locate/ijsolstr

Effect of a biasing electric field on the propagation of antisymmetric Lamb waves in piezoelectric plates

H. Liu [a], T.J. Wang [b], Z.K. Wang [b], Z.B. Kuang [a,*]

[a] *Department of Engineering Mechanics, Shanghai Jiaotong University, Shanghai 200240, China*
[b] *Department of Engineering Mechanics, Xi'an Jiaotong University, Xi'an 710049, China*

Received 21 August 2001; received in revised form 26 September 2001

Abstract

Based on the theories of anisotropic elasticity, piezoelectricity and elastic waves in solids, the propagation of antisymmetric Lamb waves in a biasing electric field is investigated in this paper. By solving the coupled differential equations of motion under a biasing electric field, the phase velocity equations of antisymmetric Lamb wave modes for electrically open and shorted cases are obtained, respectively. The beating effect arising from the difference between the phase velocity of the zero-order symmetric mode and antisymmetric mode exists in the plate when the plate has a thickness comparable to or slightly larger than the wavelength. The influence of the biasing electric field on the phase velocity, beat wavelength, mechanical displacement and stress fields for the lowest two antisymmetric modes of Lamb waves are discussed in detail. From the calculated results, it is seen that the phase velocity of the fundamental antisymmetric mode is especially sensitive to the applied biasing electric field.

Keywords: Biasing electric field; Antisymmetric Lamb waves; Phase velocity; Beating effect

1. Introduction

Acoustic devices are widely used in the fields of electric engineering, mechanical engineering, and communications, etc. Rayleigh waves, Love waves and Lamb waves are the commonly used wave modes in these acoustic devices. The behavior of the wave mode selected directly affects the performance of the device. Thus, it has great significance to study the characteristics of these waves. In vibrating piezoelectric solids small changes in acoustic wave velocity arising from a variety of causes have been exploited in the field of SAW devices and voltage sensors. The small effects may be due to biasing stresses, strains, the presence of a thin surface layer, material viscosity, mass loading, and electric fields, etc. (Tiersten, 1978). To reveal the effect of biasing states on the characteristics of waves in elastic media, Nalamwar and Epstein (1976) investigated the propagation characteristics of Rayleigh waves in a strained half-space. Also, the influence of temperature-induced biasing strains (Sinha, 1982), biasing electric fields (Kuznetsova et al., 1998),

* Corresponding author.
E-mail address: zbkuang@mail.sjtu.edu.cn (Z.B. Kuang).

0020-7683/02/$ - see front matter
PII: S0020-7683(02)00015-X

externally applied forces-induced extensional and flexural deformations (Sinha et al., 1985), and flexural biasing stress (Sinha and Tiesten, 1979) were reported on the propagation of elastic waves in anisotropic solids. Docmeci (1990) derived a set of two-dimensional approximate equations for vibrations of polarized ceramic shells under a bias. This fact is well known and widely appreciated in developing sensors for measuring different parameters such as temperature, pressure, acceleration, gas concentration and high voltages (Gatti, 1983). When a dc voltage V is applied across the electrodes, various components of stress and electric displacement are generated in the plate. These components lead to a change in the phase velocity through electroacoustic effects. With respect to mechanical biasing stresses, the magnitude of change in phase velocity due to a biasing electric is relatively great. Lamb waves are attractive owning to a higher sensitivity to the biasing electric field in comparison with Rayleigh waves (Palma et al., 1985). In addition, the Lamb wave modes that a plate supports show different electroelastic behavior, thus one has a wider choice to select a more suitable operating condition. Moreover, the zero-order antisymmetric mode (a_0) sometimes called as flexural plate wave is of especially interest due to the fact that it can be used in contact with liquids with a small attenuation (Laurent et al., 2000). In this paper, we will describe some analytical results on the propagation of the lowest two antisymmetric Lamb wave modes in the presence of a biasing electric field. The effect of a biasing electric field on the phase velocity, beat wavelength and stress fields in the infinite piezoelectric plate is discussed in detail.

2. Wave equations and boundary conditions

2.1. Static field problem

The geometry of the problem to be analyzed is shown in Fig. 1, Lamb waves propagate along the x-direction of a transversely isotropic piezoelectric plate of thickness h, with the polarization axis oriented along the z-direction. The biasing voltage is applied to the electrodes deposited on the upper surface of the plate. The electrodes on the lower surface are grounded. The biasing electric field is applied parallel to the thickness direction because a given biasing voltage can produce the largest electric field in this direction (Joshi, 1982). We assume that there exists only one constant initial stress component σ_x^0 in the plate, the other components of the initial stress are zero. All the components of initial stress and initial electric displacement should satisfy the constitutive equations in the initial configuration.

$$\sigma_x^0 = c_{11}S_x^0 + c_{12}S_y^0 + c_{13}S_z^0 - e_{31}E_z^0 \tag{1a}$$

$$\sigma_y^0 = c_{12}S_x^0 + c_{11}S_y^0 + c_{13}S_z^0 - e_{31}E_z^0 \tag{1b}$$

$$\sigma_z^0 = c_{13}S_x^0 + c_{13}S_y^0 + c_{33}S_z^0 - e_{33}E_z^0 \tag{1c}$$

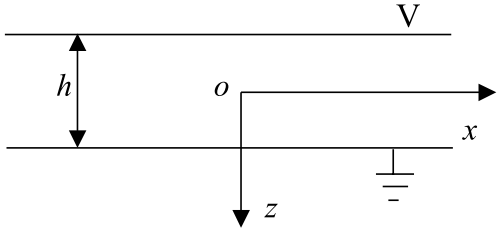

Fig. 1. Infinite piezoelectric plate in a biasing electric field.

$$D_x^0 = e_{15}S_{zx}^0 + \varepsilon_{11}E_x^0 \tag{1d}$$

$$D_y^0 = e_{15}S_{yz}^0 + \varepsilon_{11}E_z^0 \tag{1e}$$

$$D_z^0 = e_{31}S_x^0 + e_{31}S_y^0 + e_{33}S_z^0 + \varepsilon_{33}E_z^0 \tag{1f}$$

where σ_x^0, σ_y^0 and σ_z^0 are initial stresses, D_x^0, D_y^0 and D_z^0 are initial electric displacements, S_x^0, S_y^0, S_z^0, S_{zx}^0 and S_{yz}^0 are initial strains, E_x^0, E_y^0, E_z^0 are initial fields, c_{11}, c_{12}, c_{13} and c_{33} are elastic constants, e_{31}, e_{33} and e_{15} are piezoelectric constants, ε_{11} and ε_{33} are dielectric constants of the plate.

For the plain strain problem, there are no variations of any of the displacement components in the y-direction and the component of displacement in the y-direction equals to zero, thus $S_y^0 = 0$. In the case of thin plate, we have $\sigma_z^0 = 0$. From Eq. (1c), we have $S_z^0 = -(c_{13}/c_{33})S_x^0 + (e_{33}/c_{33})E_z^0$, then substituting this equation into Eqs. (1a) and (1f), one obtains

$$\begin{aligned} \sigma_x^0 &= \left(c_{11} - \frac{c_{13}^2}{c_{33}}\right)S_x^0 + \left(\frac{c_{13}e_{33}}{c_{33}} - e_{31}\right)E_z^0 \\ D_z^0 &= \left(e_{31} - \frac{c_{13}e_{33}}{c_{33}}\right)S_x^0 + \left(\frac{e_{33}^2}{c_{33}} + \varepsilon_{33}\right)E_z^0 \end{aligned} \tag{2}$$

When the biasing voltage V is applied only along the z-direction, we have $S_x^0 = 0$, $D_x^0 = D_y^0 = 0$, $\sigma_y^0 = 0$, $\tau_{xy}^0 = 0$. Because the media is an insulator, no free charge exists. The electric displacements satisfy the Gaussian equation, and the electric field E_z^0 is related to the initial electric potential φ^0, i.e.,

$$\frac{\partial D_x^0}{\partial x} + \frac{\partial D_y^0}{\partial y} + \frac{\partial D_z^0}{\partial z} = 0 \tag{3a}$$

$$E_z^0 = -\frac{\partial \varphi^0}{\partial z} \tag{3b}$$

these conditions lead to

$$\frac{\partial^2 \varphi^0}{\partial z^2} = 0 \tag{4}$$

The solution to Eq. (4) has the form $\varphi^0 = az + q$, where a and q are unknown constants, from the electrical boundary conditions on the upper surface of the plate $\varphi^0(-h/2) = V$ and the lower surface $\varphi^0(h/2) = 0$, we have

$$\varphi^0 = -\frac{V}{h}z + \frac{V}{2} \tag{5}$$

Substituting Eq. (5) into Eq. (3b), yields

$$E_z^0 = -\frac{\partial \varphi^0}{\partial z} = \frac{V}{h} \tag{6}$$

Substitution of Eq. (6) into Eq. (2) gives the initial stress and initial displacement induced by the biasing voltage

$$\begin{aligned} \sigma_x^0 &= \left(\frac{c_{13}e_{33}}{c_{33}} - e_{31}\right)\frac{V}{h} \\ D_z^0 &= \left(\frac{e_{33}^2}{c_{33}} + \varepsilon_{33}\right)\frac{V}{h} \end{aligned} \tag{7}$$

2.2. Equations of motion

The field equations of the piezoelectric body with initial stresses can be expressed as (Wang and Shang, 1997)

$$\begin{aligned} &\sigma_{ij,j} + \left(u_{i,k}\cdot\sigma^0_{kj}\right)_{,j} = \rho\cdot\ddot{u}_i \\ &D_{i,i} + \left(u_{i,j}\cdot D^0_j\right)_{,i} = 0 \end{aligned} \tag{8}$$

where $i, j, k = 1, 2, 3$; ρ is mass density; u_i and D_i denote the mechanical displacement and the electric displacement in the ith direction, respectively; σ_{ij} is stress tensor. For the plain strain problem, displacements u, v, w and electrical potential φ should satisfy $u = u(x,z,t)$, $v = 0$, $w = w(x,z,t)$, and $\varphi = \varphi(x,z,t)$ respectively. Thus Eq. (8) collapse to a much simpler set of three equations

$$\begin{aligned} &\frac{\partial\sigma_x}{\partial x} + \frac{\partial\tau_{zx}}{\partial z} + \sigma^0_x\frac{\partial^2 u}{\partial x^2} = \rho\frac{\partial^2 u}{\partial t^2} \\ &\frac{\partial\tau_{zx}}{\partial x} + \frac{\partial\sigma_z}{\partial z} + \sigma^0_x\frac{\partial^2 w}{\partial x^2} = \rho\frac{\partial^2 w}{\partial t^2} \\ &\frac{\partial D_x}{\partial x} + \frac{\partial D_z}{\partial z} + D^0_z\frac{\partial^2 u}{\partial x\partial z} + D^0_z\frac{\partial^2 w}{\partial z^2} = 0 \end{aligned} \tag{9}$$

Because of the disappearance of derivatives with respect to y, the constitutive equations of the transversely isotropic piezoelectric medium are given by

$$\begin{aligned} \sigma_x &= c_{11}S_x + c_{13}S_z - e_{31}E_z \\ \sigma_y &= c_{12}S_x + c_{13}S_z - e_{33}E_z \\ \sigma_z &= c_{13}S_x + c_{33}S_z - e_{33}E_z \\ \tau_{zx} &= c_{44}S_{zx} - e_{15}E_x \\ D_x &= e_{15}S_{zx} + \varepsilon_{11}E_x \\ D_z &= e_{31}S_x + e_{33}S_z + \varepsilon_{33}E_z \end{aligned} \tag{10}$$

where

$$\begin{aligned} &S_x = \frac{\partial u}{\partial x}, \quad S_y = \frac{\partial v}{\partial y}, \quad S_z = \frac{\partial w}{\partial z}, \quad S_{yz} = \frac{\partial w}{\partial y} + \frac{\partial v}{\partial z}, \quad S_{zx} = \frac{\partial u}{\partial z} + \frac{\partial w}{\partial x}, \quad S_{xy} = \frac{\partial u}{\partial y} + \frac{\partial v}{\partial x}, \\ &E_x = -\frac{\partial\varphi}{\partial x}, \quad E_y = -\frac{\partial\varphi}{\partial y}, \quad E_z = -\frac{\partial\varphi}{\partial z} \end{aligned}$$

Substituting Eqs. (10) and (7) into Eq. (9), one obtains the field equations in terms of the potential and the mechanical displacements

$$\begin{aligned} &\left[c_{11} + \left(\frac{c_{13}e_{33}}{c_{33}} - e_{31}\right)\frac{V}{h}\right]\frac{\partial^2 u}{\partial x^2} + c_{44}\frac{\partial^2 u}{\partial z^2} + (c_{13}+c_{44})\frac{\partial^2 w}{\partial x\partial z} + (e_{31}+e_{15})\frac{\partial^2\varphi}{\partial x\partial z} = \rho\frac{\partial^2 u}{\partial t^2} \\ &(c_{13}+c_{44})\frac{\partial^2 u}{\partial x\partial z} + \left[c_{44} + \left(\frac{c_{13}e_{33}}{c_{33}} - e_{31}\right)\frac{V}{h}\right]\frac{\partial^2 w}{\partial x^2} + c_{33}\frac{\partial^2 w}{\partial z^2} + e_{15}\frac{\partial^2\varphi}{\partial x^2} + e_{33}\frac{\partial^2\varphi}{\partial z^2} = \rho\frac{\partial^2 w}{\partial t^2} \\ &\left[e_{15} + e_{31} + \left(\frac{e^2_{33}}{c_{33}} + \varepsilon_{33}\right)\frac{V}{h}\right]\frac{\partial^2 u}{\partial x\partial z} + e_{15}\frac{\partial^2 w}{\partial x^2} + \left[e_{33} + \left(\frac{e^2_{33}}{c_{33}} + \varepsilon_{33}\right)\frac{V}{h}\right]\frac{\partial^2 w}{\partial z^2} - \varepsilon_{11}\frac{\partial^2\varphi}{\partial x^2} - \varepsilon_{33}\frac{\partial^2\varphi}{\partial z^2} = 0 \end{aligned} \tag{11}$$

The potential φ_0 in the region outside the plate must satisfy Laplace's equation,

$$\frac{\partial^2\varphi_0}{\partial x^2}+\frac{\partial^2\varphi_0}{\partial z^2}=0 \tag{12}$$

2.3. Assumed solutions of antisymmetric Lamb wave modes (EPS)

Lamb waves with variations of w symmetric and u antisymmetric about the central plane are called antisymmetric modes (even potential state, EPS). EPS modes correspond to the flexural vibrations of the plate. Thus the solutions are assumed to have the form (Romos and Otero, 1997)

$$\begin{aligned} u &= B_1\sin(kbz)\exp[\mathrm{i}k(x-ct)]\\ w &= B_2\cos(kbz)\exp[\mathrm{i}k(x-ct)]\\ \varphi &= B_3\cos(kbz)\exp[\mathrm{i}k(x-ct)] \end{aligned} \tag{13}$$

where B_1, B_2 and B_3 are amplitudes of each partial wave. k is wave number and $k=2\pi/\lambda$, λ is wavelength, c is the phase velocity, b is the propagation constant of the partial wave along the normal to the layer, $\mathrm{i}=\sqrt{-1}$.

Substituting Eq. (13) into Eq. (11), we have

$$\begin{aligned} &\left[c_{11}-\rho c^2+c_{44}b^2+\left(\frac{c_{13}e_{33}}{c_{33}}-e_{31}\right)\frac{V}{h}\right]B_1+(c_{13}+c_{44})b\mathrm{i}B_2+(e_{31}+e_{15})b\mathrm{i}B_3=0\\ &(c_{13}+c_{44})b\mathrm{i}B_1-\left[c_{44}-\rho c^2+c_{33}b^2+\left(\frac{c_{13}e_{33}}{c_{33}}-e_{31}\right)\frac{V}{h}\right]B_2-(e_{15}+e_{33}b^2)B_3=0\\ &\left[e_{15}+e_{31}+\left(\frac{e_{33}^2}{c_{33}}+\varepsilon_{33}\right)\frac{V}{h}\right]b\mathrm{i}B_1-\left\{e_{15}+\left[e_{33}+\left(\frac{e_{33}^2}{c_{33}}-e_{31}\right)\frac{V}{h}\right]b^2\right\}B_2+(\varepsilon_{11}+\varepsilon_{33}b^2)B_3=0 \end{aligned} \tag{14}$$

In order to get a nontrivial solution, the determinant of the square matrix must be equal to zero. This condition results in a third-order equation in b^2 with phase velocity c as the unknown parameter. For every value of c, biasing voltage V and material constants, there are three solutions b_l^2 ($l=1$–3). On account of the form of Eq. (13), the roots $+b_l$ and $-b_l$ do not yield independent solutions. So only three solutions of b_l ($l=1$–3) are adopted. Substitution of b_l ($l=1$–3) into any two of Eq. (14) yields the amplitude ratios B_{1l}/B_{3l} and B_{2l}/B_{3l} ($l=1$–3), i.e.,

$$\begin{aligned} B_{1l} &= F_{1l}B_{3l}\\ B_{2l} &= F_{2l}B_{3l} \end{aligned} \tag{15}$$

where

$$F_{1l}=\frac{(e_{31}+e_{15})\cdot\left[c_{44}-\rho c^2+c_{33}b_l^2+\left(\frac{c_{13}e_{33}}{c_{33}}-e_{31}\right)\frac{V}{h}\right]-(e_{15}+e_{33}b_l^2)(c_{13}+c_{44})}{-\left[c_{11}-\rho c^2+c_{44}b_l^2+\left(\frac{c_{13}e_{33}}{c_{33}}-e_{31}\right)\frac{V}{h}\right]\left[c_{44}-\rho c^2+c_{33}b_l^2+\left(\frac{c_{13}e_{33}}{c_{33}}-e_{31}\right)\frac{V}{h}\right]+(c_{13}+c_{44})^2b_l^2}b_l\cdot\mathrm{i}$$

$$F_{2l}=\frac{\left[c_{11}-\rho c^2+c_{44}b_l^2-\left(\frac{c_{13}e_{33}}{c_{33}}+e_{31}\right)\frac{V}{h}\right](e_{15}+e_{33}b_l^2)-(c_{13}+c_{44})(e_{31}+e_{15})b_l^2}{-\left[c_{11}-\rho c^2+c_{44}b_l^2+\left(\frac{c_{13}e_{33}}{c_{33}}-e_{31}\right)\frac{V}{h}\right]\left[c_{44}-\rho c^2+c_{33}b_l^2+\left(\frac{c_{13}e_{33}}{c_{33}}-e_{31}\right)\frac{V}{h}\right]+(c_{13}+c_{44})^2b_l^2}$$

Substituting Eq. (15) into Eq. (13), the solutions of displacements and electrical potential for EPS are expressed as

$$\begin{aligned} u &= \sum_{l=1}^{3} F_{1l} B_{3l} \sin(k b_l z) \exp[\mathrm{i}k(x-ct)] \\ w &= \sum_{l=1}^{3} F_{2l} B_{3l} \cos(k b_l z) \exp[\mathrm{i}k(x-ct)] \\ \varphi &= \sum_{l=1}^{3} B_{3l} \cos(k b_l z) \exp[\mathrm{i}k(x-ct)] \end{aligned} \tag{16}$$

The solutions for electrical potential in the vacuum can be obtained from Eq. (12), i.e.,

$$\varphi_0 = B_4 \mathrm{e}^{-kz} \exp[\mathrm{i}k(x-ct)] \quad (z \geqslant h/2) \tag{17}$$

2.4. Boundary conditions

The particle displacements and the traction components of stress must be continuous across the interface between two different materials. In the case under investigation, the traction components of stress at the surfaces must vanish. The electrical boundary conditions are provided by the continuity of the potential and of the normal component of electric displacement across the free surfaces (Farnell and Adler, 1972). Thus the boundary conditions on the solutions of Eqs. (16) and (17) are listed as follows:

(i) The mechanical traction-free conditions at $z = \pm h/2$

$$\tau_{zx}(x,\ \pm h/2) = 0$$
$$\sigma_z(x,\ \pm h/2) = 0$$

(ii) The electrical boundary conditions for electrically open case at $z = \pm h/2$

$$\varphi_0(x,\ \pm h/2) = \varphi(x,\ \pm h/2)$$
$$D_{z0}(x,\ \pm h/2) = D_z(x,\ \pm h/2)$$

(iii) The electrical boundary conditions for electrically shorted case at $z = \pm h/2$

$$\varphi(x,\ \pm h/2) = 0$$

3. Solutions of the phase velocity

3.1. Electrically open case

Evaluating the mechanical and electrical boundary conditions (i) and (ii), and taking into account solutions (16) and (17) respectively, we can obtain a set of four homogeneous algebraic equations in the unknown constants B_{31}, B_{32}, B_{33} and B_4. After simplifying, we can obtain the algebraic equations in the unknown constants B_{31}, B_{32} and B_{33} i.e.,

$$[P][B] = 0 \tag{18}$$

where $[P]$ is a 3×3 matrix, P_{sl} $(s = 1\text{–}3, l = 1\text{–}3)$ are

$$P_{1l} = [c_{44}(F_{2l} \cdot \mathrm{i} + b_l F_{1l}) + e_{15} \cdot \mathrm{i}] \cos\left(kb_l \frac{h}{2}\right)$$

$$P_{2l} = (c_{13}F_{1l} \cdot \mathrm{i} - c_{33}b_l F_{2l} - e_{33}b_l) \sin\left(kb_l \frac{h}{2}\right)$$

$$P_{3l} = \frac{1}{\varepsilon_0}(e_{31}F_{1l} \cdot \mathrm{i} - e_{33}b_l F_{2l} + \varepsilon_{33}b_l) \sin\left(kb_l \frac{h}{2}\right) - \cos\left(kb_l \frac{h}{2}\right)$$

where ε_0 is the dielectric constant of air.

Let

$$d_1 = c_{44}(F_{21} \cdot \mathrm{i} + b_1 F_{11}) + e_{15} \cdot \mathrm{i}, \quad d_2 = c_{44}(F_{22} \cdot \mathrm{i} + b_2 F_{12}) + e_{15} \cdot \mathrm{i},$$
$$d_3 = c_{44}(F_{23} \cdot \mathrm{i} + b_3 F_{13}) + e_{15} \cdot \mathrm{i}, \quad f_1 = c_{13}F_{11} \cdot \mathrm{i} - c_{33}b_1 F_{21} - e_{33}b_1,$$
$$f_2 = c_{13}F_{12} \cdot \mathrm{i} - c_{33}b_2 F_{22} - e_{33}b_2, \quad f_3 = c_{13}F_{13} \cdot \mathrm{i} - c_{33}b_3 F_{23} - e_{33}b_3,$$
$$g_1 = \frac{1}{\varepsilon_0}(e_{31}F_{11} \cdot \mathrm{i} - e_{33}b_1 F_{21} + \varepsilon_{33}b_1), \quad g_2 = \frac{1}{\varepsilon_0}(e_{31}F_{12} \cdot \mathrm{i} - e_{33}b_2 F_{22} + \varepsilon_{33}b_2),$$
$$g_3 = \frac{1}{\varepsilon_0}(e_{31}F_{13} \cdot \mathrm{i} - e_{33}b_3 F_{23} + \varepsilon_{33}b_3)$$

Then the phase velocity equation is obtained when the determinant of $|P|$ in Eq. (18) vanishes, i.e.,

$$ctg(\pi m b_1)[e_1 ctg(\pi m b_2) - h_1] + ctg(\pi m b_2)[e_3 ctg(\pi m b_3) - h_2] + ctg(\pi m b_3)[e_2 ctg(\pi m b_1) - h_3] = 0 \tag{19}$$

where

$$m = h/\lambda, \quad e_1 = f_3(d_2 - d_1), \quad e_2 = f_2(d_1 - d_3), \quad e_3 = f_1(d_3 - d_2), \quad h_1 = d_1(f_2 g_3 - f_3 g_2),$$
$$h_2 = d_2(f_3 g_1 - f_1 g_3), \quad h_3 = d_3(f_1 g_2 - f_2 g_1)$$

m is a ratio of plate thickness to wavelength. It is a very important variable in acoustic wave devices, the wave modes that a plate supports depend on the value of the ratio h/λ. Generally, Lamb waves are excited by an interdigital transducer (IDT) deposited on the piezoelectric plate. The wavelength λ equals to the spatial periodicity of the IDTs. Also, the thickness of the plate can be accurately measured. Thus the value of m can be defined.

In addition, for the electrically open case, the biasing voltage V should be equal to zero.

3.2. Electrically shorted case

In a similar way to the electrically open case, we obtain the phase velocity equation for the electrically shorted case, i.e.,

$$e_1 ctg(\pi m b_1) ctg(\pi m b_2) + e_2 ctg(\pi m b_1) ctg(\pi m b_3) + e_3 ctg(\pi m b_2) ctg(\pi m b_3) = 0 \tag{20}$$

4. Solutions of stress fields

After the root of the phase velocity is found, for both electrically open and shorted cases, from the first two equations of the boundary equations, we obtain the amplitude ratios

$$B_{31} = \beta_1 B_{33}, \quad B_{32} = \beta_2 B_{33}, \quad B_{33} = \beta_3 B_{33} \tag{21}$$

where

$$\beta_1 = \frac{-\cos(\pi m b_3) d_3 \sin(\pi m b_2) f_2 + \cos(\pi m b_2) d_2 \sin(\pi m b_3) f_3}{\cos(\pi m b_1) d_1 \sin(\pi m b_2) f_2 - \cos(\pi m b_2) d_2 \sin(\pi m b_1) f_1}$$

$$\beta_2 = \frac{-\cos(\pi m b_1) d_1 \sin(\pi m b_3) f_3 + \cos(\pi m b_3) d_3 \sin(\pi m b_1) f_1}{\cos(\pi m b_1) d_1 \sin(\pi m b_2) f_2 - \cos(\pi m b_2) d_2 \sin(\pi m b_1) f_1}$$

$$\beta_3 = 1$$

The value of B_{33} is determined by the excitation.

Substituting Eq. (21) into Eq. (16), we have

$$\begin{aligned} u &= \left[\sum_{l=1}^{3} F_{1l}\beta_l \sin(kb_l z)\right] B_{33} \exp[\mathrm{i}k(x-ct)] \\ w &= \left[\sum_{l=1}^{3} F_{2l}\beta_l \cos(kb_l z)\right] B_{33} \exp[\mathrm{i}k(x-ct)] \\ \varphi &= \left[\sum_{l=1}^{3} \beta_l \cos(kb_l z)\right] B_{33} \exp[\mathrm{i}k(x-ct)] \end{aligned} \tag{22}$$

Substituting Eq. (22) into the constitutive equations, the stress fields for EPS can be expressed as

$$\begin{aligned} \tau_{zx} &= \left\{\sum_{l=1}^{3} [c_{44}(F_{2l}\cdot \mathrm{i} + b_l F_{1l}) + e_{15}\cdot \mathrm{i}] k\beta_l \cos(kb_l z)\right\} kB_{33} \exp[\mathrm{i}k(x-ct)] \\ \sigma_z &= \left[\sum_{l=1}^{3} (c_{13}F_{1l}\cdot \mathrm{i} - c_{33}b_l F_{2l} - e_{33}b_l) k\beta_l \sin(kb_l z)\right] kB_{33} \exp[\mathrm{i}k(x-ct)] \\ \sigma_x &= \left[\sum_{l=1}^{3} (c_{11}F_{1l}\cdot \mathrm{i} - c_{13}b_l F_{2l} - e_{31}b_l) k\beta_l \sin(kb_l z)\right] kB_{33} \exp[\mathrm{i}k(x-ct)] \\ \sigma_y &= \left[\sum_{l=1}^{3} (c_{12}F_{1l}\cdot \mathrm{i} - c_{13}b_l F_{2l} - e_{31}b_l) k\beta_l \sin(kb_l z)\right] kB_{33} \exp[\mathrm{i}k(x-ct)] \end{aligned} \tag{23}$$

5. Discussion

The effect curves of a biasing electric field on the phase velocity, displacements, and stress fields of the first two antisymmetric Lamb wave modes are given. Calculations are performed for PZT-5H ceramics. The material constants of PZT-5H ceramics are taken from Ristic (1983), as shown in Table 1. The dielectric constant of vacuum is $\varepsilon_0 = 8.85 \times 10^{-12}$ F/m. We assume the plate thickness $h = 0.5$ mm, to display the amplitudes of mechanical displacements and stress components as a function of z, the real part of their expressions are plotted (Mesquida et al., 1998). Let χ denote all these variables, then

$$\chi(x,z,t) = \bar{\chi}(z)\exp[\mathrm{i}k(x-ct)]$$

This leads to

$$\mathrm{Re}[\chi(x,z,t)] = \sqrt{\{\mathrm{Re}[\bar{\chi}(z)]\}^2 + \{\mathrm{Im}[\bar{\chi}(z)]\}^2} \times \cos[k(x-ct)+\alpha]$$

Table 1
Material constants

Material	Elastic constant (10^{10} N/m^2)					Mass density ρ (kg/m^3)	Piezoelectric constant (C/m^2)			Dielectric constant (10^{-10} F/m)	
	c_{11}	c_{12}	c_{13}	c_{33}	c_{44}		e_{15}	e_{31}	e_{33}	ε_{11}	ε_{33}
PZT-5H ceramics	12.1	7.95	8.41	11.7	2.30	7.5	17.0	−6.5	23.3	150	130
PZT-2 ceramics	13.5	6.79	6.81	11.3	2.22	7.6	9.8	−1.9	9.0	44.6	23.0
Lead–oxide glass	6.13				2.18	3.879				0.36	0.36
SiO_2 glass	7.85				3.12	2.2				0.33	0.33
Borosilicate glass	7.42				2.78	2.23				0.45	0.45
ZnO	20.96	12.11	10.51	21.09	4.25	5.68	−0.48	−0.573	1.32	0.75	0.90

where

$$\alpha = arctg\left(\frac{\mathrm{Im}[\bar{\chi}(z)]}{\mathrm{Re}[\bar{\chi}(z)]}\right)$$

Generally, we plot $\mathrm{Im}[\bar{\chi}(z)]$ and $\mathrm{Re}[\bar{\chi}(z)]$ to show the z dependence of the amplitude of χ.

Effect of the biasing electric field on the fractional phase velocity change $\Delta c/c$ is shown in Figs. 2 and 3. Here $\Delta c = c_{\mathrm{bias}} - c_{\mathrm{un}}$, c_{bias} is the phase velocity in a biasing state and c_{un} in an unbiased state. m is the ratio of plate thickness to wavelength, a very important parameter for SAW, changes from 0.01 to 3. The breakdown fields of ceramics are of the order of 4–60 kV/mm (Xu, 1993). We assume the plate is under a biasing electric field of 2.5 kV/mm without breakdown. Fig. 2(a) and (b) illustrates the effects on the a_0 Lamb wave mode. It appears in Fig. 2 that the biasing electric field has great effect on the phase velocity of the a_0 mode. The phase velocity increases when the biasing electric field changes from −2.5 to 2.5 kV/mm. As a matter of fact, at $m = 0.01$, the phase velocity approaches zero when the biasing electric field is less than −1.35 kV/mm, then increases remarkably when the biasing electric field increases to 2.5 kV/mm. Thus the fractional velocity change due to the biasing state is especially great and of the order of −0.92 to 0.68. From Fig. 2(b), it is seen that for larger m, the phase velocity of the a_0 mode increases slowly in comparison with Fig. 2(a). The fractional velocity change ranges from 0.09% (at $m = 3.00$) to 0.2% (at $m = 0.30$). From inspection of Fig. 3, it can be observed that the phase velocity of the a_1 mode also changes as a function of the biasing electric field. The fractional phase velocity change is maximally increased by 0.0697% at about $m = 3.00$. In conclusion, we will say that the a_0 mode is higher sensitive to the biasing electric field in comparison with the a_1 mode. The sensitivity of the a_0 mode increases when the ratio of plate thickness to wavelength reduces. This feature is applicable to build sensors able to operate in liquids. Velocities of Lamb

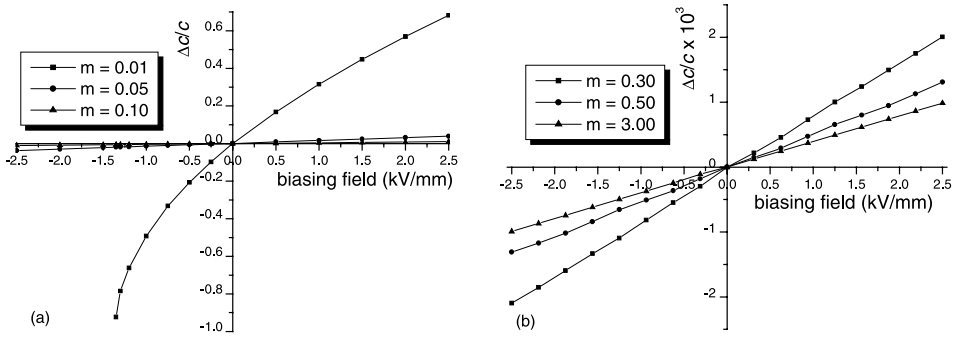

Fig. 2. Relations between the fractional phase velocity change of the a_0 mode and the biasing electric field for electrically shorted case.

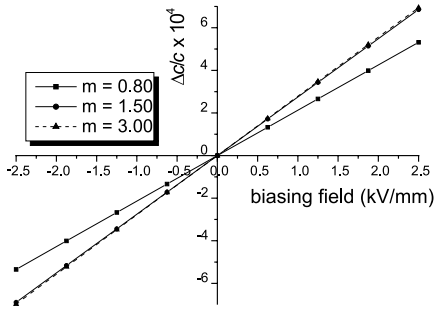

Fig. 3. Relations between the fractional phase velocity change of the a_1 mode and the biasing electric field for electrically shorted case.

wave modes a_0 and a_1 for electrically open case ($V = 0$) as a function of k are shown in Fig. 4. From Fig. 4, it is seen that with increasing the value of k, the velocity for the a_0 mode approaches closely to the free-surface Rayleigh velocity, the velocity of the a_1 mode approaches to the bulk shear velocity.

For a plate with finite thickness comparable to the wavelength, a surface wave on the upper boundary has a small residual amplitude at the lower boundary and vise versa. These small residual amplitudes cause a continuous coupling between the two fundamental symmetric (s_0) and antisymmetric (a_0) Lamb waves (Auld, 1973). Due to the difference in velocities between the two coupled modes, the beating effect exist in plate, which has been manifested by experiments (Joshi and Jin, 1991). Suppose that at a certain point x_0, the a_0 and s_0 modes are in phase with each other, thus corresponding to a SAW on the top surface of the plate. Let c_a and c_s denote the phase velocities of the a_0 and s_0 modes, respectively, the phase shifts between the modes will be expressed by $\theta = 2\pi f(L/c_a - L/c_s) = 2\pi L/L_b$, where L is the traveling distance, f is the frequency of the wave, and $L_b = c_a\lambda/(c_s - c_a)$ is the beat wavelength. If $L = L_b/2$, there will be a 180° phase shift between the a_0 and s_0 modes. Then the energy will be transferred to the bottom surface of the plate. After traveling an additional $L_b/2$, the energy will be transferred back to the top of the plate, thus the beating effect appears as a sinusoidal function of the distance traveled. SAW oscillator vapor sensors can take advantage of this well-known property of beating effect (Chuang and White, 1982). In these sensors, the polymer able to absorb vapors is located on the lower surface where the energy reaches it, the phase velocity can be affected and frequency shifts. The energy ultimately returns to the upper surface where a transducer can detect it. In a biasing electric field, the phase velocities of the a_0 and s_0 modes are modified differently by the electric field, so the beating effect is also affected by the biasing electric field. Thus the locations of the polymers and transducers may be changed. In Fig. 5(a), the variations of beat wavelength L_b with different values of h/λ are plotted. The horizontal axis is the ratio of plate thickness to wavelength,

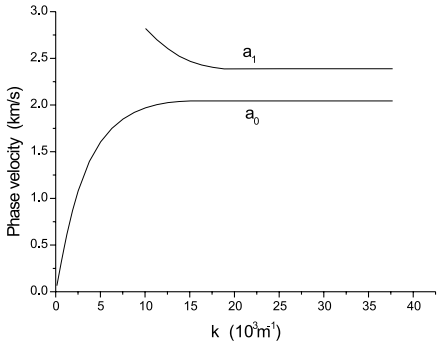

Fig. 4. Dispersion relations for the a_0 mode and a_1 mode for electrically open case.

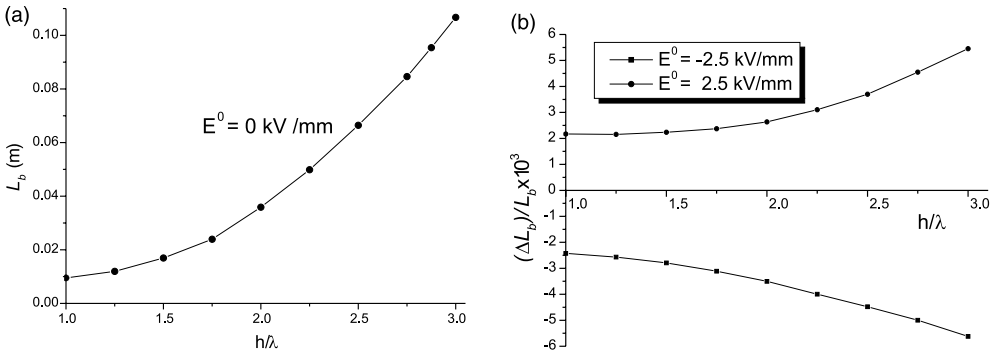

Fig. 5. Variations of the beat wavelength vs. the biasing electric field: (a) L_b, (b) $\Delta L_b/L_b$.

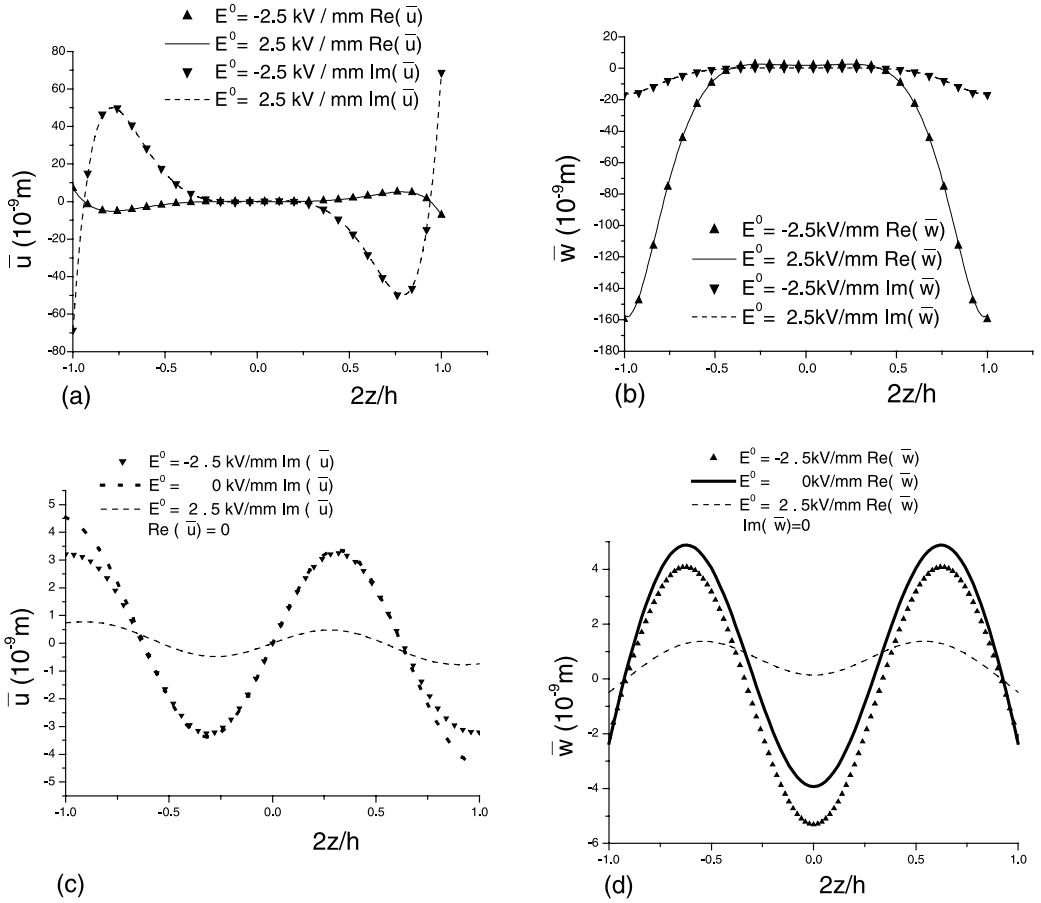

Fig. 6. At $m = 3.0$, variations of particle displacement along thickness of the PZT-5H plate: (a) $\bar{u}$ of the a_0 mode, (b) $\bar{w}$ of the a_0 mode, (c) $\bar{u}$ of the a_1 mode and (d) $\bar{w}$ of the a_1 mode.

starting from 1.0. The vertical axis is the beat wavelength. It is found that as h/λ increases, the velocity difference between the a_0 and s_0 modes decreases, the beat wavelength increases evidently. From the fractional change in beat wavelength $\Delta L_b/L_b$ shown in Fig. 5(b), it can be seen that for the same value of h/λ, the beat wavelength of the negative biasing electric field is smaller than that of the unbiased state, the beat wavelength of the unbiased state is smaller than that of the positive electric field. The maximum fractional change in beat wavelength is 0.562% corresponding to a biasing electric field of -2.5 kV/mm at $m = 3.00$.

Effects of the biasing electric field on the displacements of antisymmetric Lamb wave modes are shown in Fig. 6. The horizontal axis is the depth into the material, $2z/h = -1$ corresponds to the top surface of the plate and $2z/h = 1$ bottom surface of the plate. From Fig. 6, we note that for $m = 3.0$, a relative large ratio of plate thickness to wavelength, the biasing electric field has no effect on the displacement components of the a_0 modes, but has some effects on the a_1 modes. For the same excitation, it is obviously seen that the displacement amplitudes $|u|$ of the a_1 mode under unbiased states are always larger than that of the biased states along the plate thickness.

The stress components of the antisymmetric Lamb wave modes in a biasing electrical field are plotted for $m = 3.0$ in Fig. 7. From Fig. 7, it is seen that σ_x, σ_y, and σ_z are antisymmetric, τ_{zx} is symmetric with respect to the center plane for the a_0 mode. The biasing electric field has no effect on the stress distribution (except σ_x) for the a_0 mode.

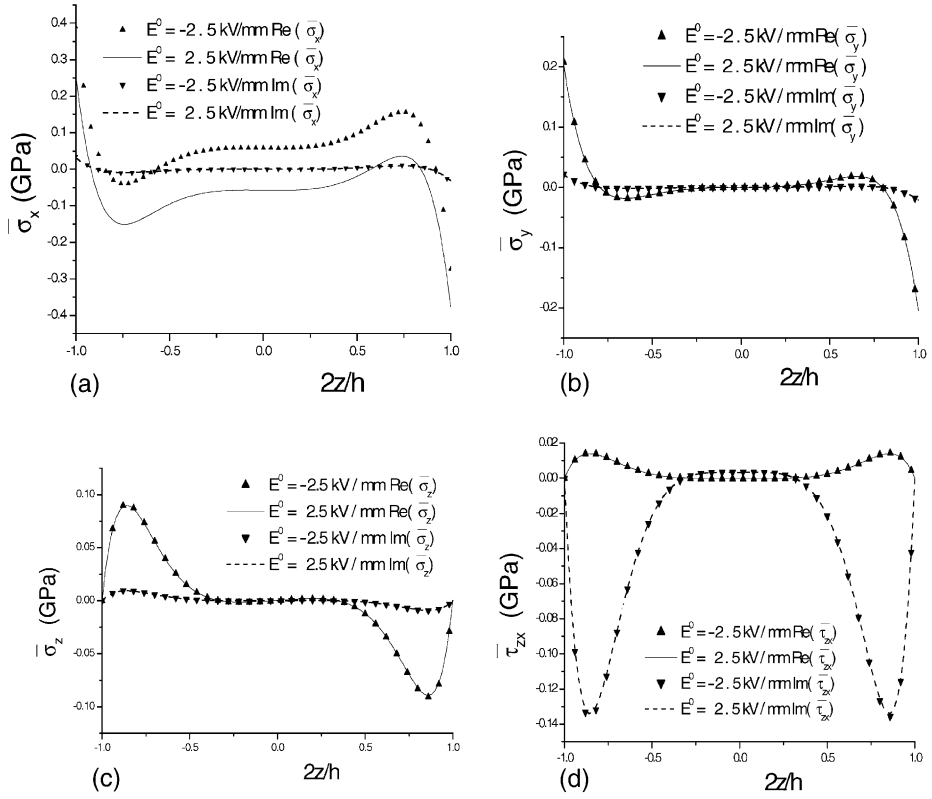

Fig. 7. At $m = 3.0$, variations of stress fields of the a_0 mode along thickness of the PZT-5H plate: (a) $\bar{\sigma}_x$, (b) $\bar{\sigma}_y$, (c) $\bar{\sigma}_z$, (d) $\bar{\tau}_{zx}$.

6. Conclusions

In recent years, there has been a growing interest in using Lamb waves for a variety of sensor applications. This paper has presented a theoretical analysis of the propagation of antisymmetric Lamb waves in a biasing electric field. It is evident that the phase velocity of the antisymmetric Lamb wave modes is sensitive to the biasing electric field. By applying an electric field near the breakdown field of the medium, the fractional velocity change for the a_0 mode in the case of relatively large ratios of plate thickness to wavelength ranges from 0.09% to 0.2%. The zero-order antisymmetric Lamb wave mode is the most sensitive compared to other modes. Reducing the ratio of the plate thickness to wavelength can enhance the sensitivity. This feature is applicable to build high-performance sensors in contact with liquids. When the plate has a thickness comparable to or slightly larger than the wavelength, the beating effect is found in the plate. The beat wavelength increases when applying a positive biasing voltage, and decreases when applying a negative biasing voltage. This property can be used to accurately fabricate a sensor for an enhanced performance. It is shown that the displacement and stress fields of antisymmetric Lamb wave modes can also be affected by a biasing electric field. The detailed effects are relevant to the specified Lamb wave modes.

The method applied in the present paper seems to be relatively simple and could be used in the study of acoustic waves along other analogous systems. Experimental works on different piezoelectric material should be simulated and compared to the analytical research.

Acknowledgement

This work is supported by the National Natural Science Foundation through Grants no. 10132010 and 10072033.

References

Auld, B.A., 1973. Acoustic Field and Waves in Solids. Wiley, New York, pp. 93–94.

Chuang, C.T., White, R.M., 1982. A thin-membrane surface-acoustic-wave vapor-sensing device. IEEE Electr. Dev. Lett. EDL-3, 145–147.

Docmeci, M.C., 1990. Shell theory for vibrations of piezoelectric ceramics under a bias. IEEE Trans. Ultrason. Ferro. Fre. Control 37, 369–385.

Farnell, G.W., Adler, E.L., 1972. Elastic wave propagation in thin layers. In: Physical Acoustics IX. Academic Press, New York and London, pp. 35–127.

Gatti, E., 1983. A surface acoustic wave voltage sensor. Sensors and Actuator. 4, 45–54.

Joshi, S.G., Jin, Y., 1991. Propagation of ultrasonic Lamb waves in piezoelectric plates. J. Appl. Phys. 70, 4113–4120.

Joshi, S.G., 1982. Surface acoustic wave propagation in a biasing electric field. J. Acoust. Soc. Am. 72, 1872–1878.

Kuznetsova, I.E., Zaitsev, B.D., Polyakov, P.V., Mysenko, M.B., 1998. External electric field effect on the properties of Bleustein–Gulyaev surface acoustic waves in lithium niobate and strontium titanate. Ultrasonics 36, 431–434.

Laurent, T., Bastien, F.O., Pommier, J.C., Cachard, A., Remiens, D., Cattan, E., 2000. Lamb wave and plate mode in ZnO/silicon and AIN/silicon membrane application to sensors able to operate in contact with liquid. Sensors Actuator. A 87, 26–37.

Mesquida, A.A., Otero, J.A., Ramos, R.R., Comas, F., 1998. Wave propagation in layered piezoelectric structrues. J. Appl. Phys. 83, 4652–4659.

Nalamwar, A.L., Epstein, M., 1976. Surface acoustic waves in strained media. J. Appl. Phys. 47, 43–48.

Palma, A., Palmieri, L., Socino, G., Verona, E., 1985. Lamb-wave electroacoustic voltage sensor. J. Appl. Phys. 58, 3265–3267.

Ristic, V.M., 1983. Principles of Acoustic Devices. Wiley, New York, p. 47, 198.

Romos, R.R., Otero, J.A., 1997. Wave propagation in a piezoelectric layer. J. Appl. Phys. 81, 7242–7247.

Sinha, B.K., 1982. Elastic waves in crystals under a bias. Ferroelectrics 41, 61–73.

Sinha, B.K., Tanski, W.J., Lukaszek, T., Ballato, A., 1985. Influence of biasing stresses on the propagation of surface waves. J. Appl. Phys. 57, 767–776.

Sinha, B.K., Tiesten, H.F., 1979. On the influence of flexural biasing state on the velocity of piezoelectric surface waves. Wave motion 1, 37–51.

Tiersten, T., 1978. Perturbation theory for linear electroelastic equations for small fields superposed on a bias. J. Acoust. Soc. Am. 64, 832–837.

Wang, Z.K., Shang, F.L., 1997. Cylindrical bulking of piezoelectric laminated plates. Acta Mech. Solida Sinica 18, 101–108.

Xu, Y.X., 1993. Electronic Ceramic Materials. Tian Jin University Press, p. 13.